Methane-to-Methanol Conversion by Gas-Phase Transition Metal Oxide Cations: Experiment and Theory

Ricardo B. Metz

Department of Chemistry, University of Massachusetts, Amherst, MA 01003 USA

Abstract

Gas-phase transition metal oxide cations can convert methane to methanol. Methane activation by MO^+ is discussed in terms of thermodynamics, the electronic structure of MO^+ and the mechanism for the reaction. Features of the potential energy surface that determine the efficiency and selectivity of the reaction are identified and related to the rich experimental literature. Photodissociation spectra of intermediates of the $FeO^+ + CH_4$ reaction are also presented.

Introduction

The direct oxidation of methane to an easily transportable liquid such as methanol has attracted great experimental and theoretical interest due to its importance as an industrial process and as the simplest model for alkane oxidation.(1-3) Although no direct, efficient methane-methanol conversion scheme has yet been developed,(1) significant advances have been made using iron-containing catalysts. Wang and Otsuka have studied the direct oxidation of methane to methanol using an $FePO_4$ catalyst and N_2O and H_2/O_2 as the oxidizing agents.(4, 5) Despite the high catalytic selectivity obtained for methanol production, the reaction yield is low. Other approaches that have achieved modest success include direct oxidation by nitrous oxide in a plasma,(6) oxidation of methane to a methyl ester with a platinum catalyst,(7) and direct methane-methanol conversion using an iron-doped zeolite.(8) In biological systems methane-methanol conversion occurs efficiently and is catalyzed by the enzyme methane monooxygenase (MMO), which contains non-heme iron centers in the active site.(9-11)

In 1990 Schröder and Schwarz reported that gas-phase FeO^+ directly and efficiently converts methane to methanol.(12) Reactions of gas-phase transition metal oxides with methane are thus a simple model system for the direct conversion of methane to methanol that is sufficiently small to be amenable to detailed experimental and theoretical study. As a result these reactions have been extensively studied.

Thermodynamic Considerations and the Electronic Structure of MO^+

The partial oxidation of methane to methanol

$$\tfrac{1}{2} O_2 + CH_4 \rightarrow CH_3OH \qquad (1)$$

is exothermic by 126 kJ/mol.(13) (For consistency all thermodynamics in this article are at 0 Kelvin). In its simplest form, the catalytic conversion of methane to methanol by M^+/MO^+ can be written as

$$M^+ + \tfrac{1}{2} O_2 \rightarrow MO^+ \qquad (2)$$
$$MO^+ + CH_4 \rightarrow M^+ + CH_3OH \qquad (3)$$

Reaction 2 is exothermic if $D_o(M^+\text{-}O) > 249$ kJ/mol, and reaction 3 is exothermic if $D_o(M^+\text{-}O) < 375$ kJ/mol. Figure 1 shows M^+-O bond strengths for the transition metals. Values are from Armentrout(14) for the first-row metals and from Schröder et al.(15) for the second- and third-row metals, except for platinum.(16) Metals with values of $D_o(M^+\text{-}O)$ within the limits imposed by reactions 2 and 3 (dashed lines in the figure) are in bold. The early transition metals bind so strongly to oxygen that reaction with methane is endothermic, while some of the late transition metals bind oxygen so weakly that
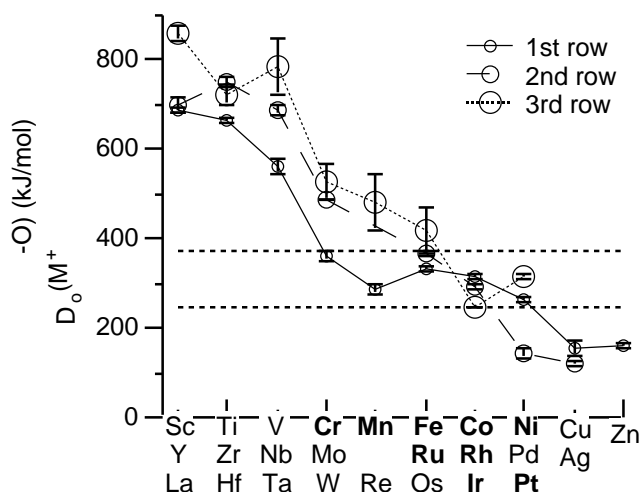
Figure 1: M^+-O bond strengths

reaction 2 is endothermic, although MO^+ may react efficiently with methane.

The electronic structure of MO^+ has been the subject of numerous theoretical studies. Most of these studies are covered in Harrison's excellent review article.[17] Detailed descriptions of bonding in the first-row transition metal MO^+ have been given by Carter and Goddard,[18] Fiedler et al.,[19] Bauschlicher and coworkers[20] and, recently, by Nakao et al.[21] The reactions of FeO^+ and PtO^+ are especially interesting, and these ions have been studied in detail by Fiedler et al.[22] and Heinemann et al.[23] Coordinatively unsaturated compounds containing transition metals tend to have many low-lying excited electronic states. Recently, time dependent density functional (TD-DFT) calculations have emerged as a surprisingly accurate, efficient way to characterize excited states. Following Borowski and Broclawik's study[24] of neutral VO and MoO, we have investigated FeO^+ [25, 26] and PtO^+ [27] using TD-DFT, obtaining results in excellent agreement with experiment.

In contrast to the large numbers of experimental studies of *reactions* of MO^+, there have been few studies of their spectroscopy. Photoelectron spectroscopy of the neutral oxides is challenging, due to the high temperatures required to produce a useful vapor pressure, but has been used by Dyke and coworkers to investigate VO^+, CrO^+, NbO^+ and TaO^+ with vibrational resolution.[28-30] Weisshaar and coworkers used a laser ablation source to produce a cold molecular beam of refractive molecules and REMPI pulsed field ionization to obtain rotationally resolved photoelectron spectra of TiO and VO, measuring rotational constants of the corresponding ions.[31, 32]

More recently, photodissociation has emerged as a powerful tool for studying these ions. We have studied predissociation of a ^{6} -^{6} band of FeO^+ which has a lifetime-limited linewidth of 1.5 cm^{-1}[33] and have recently obtained spectra of several bands in PtO^+.[27] For higher resolution studies, resonant two-photon dissociation is very promising, as the resolution is typically limited by the laser linewidth to ~0.05 cm^{-1}. Brucat and coworkers[34] demonstrated the power of this technique in their study of ^{5} $_5$-^{5} $_4$ and ^{5} $_3$-^{5} $_4$ transitions in CoO^+ and our group[25, 26] and Brucat's group[35] have recently applied it to a ^{6} - ^{6} transition in FeO^+. In each case, detailed analysis of the rotationally resolved spectrum gives bond lengths and a wealth of rotational constants.

Figure 2 shows schematic molecular orbitals and occupancies for several of the first row MO^+, based on the experiments and calculations described above. The 7 orbital is basically the oxygen 2s orbital; the 8 is formed by combining the $3d_{z^2}$ on the metal with $2p_z$ on oxygen (the primary contributor); and the 3 orbitals result from metal $3d_{xz}$ + oxygen $2p_x$ and metal $3d_{yz}$ + oxygen $2p_y$. All of these orbitals are filled in ScO^+, which has a very strong bond, as the 7 is nonbonding, while the 8 and two 3 orbitals are strongly bonding. The remaining orbitals shown are at similar energies and tend to fill so as to maximize the number of unpaired electrons. The 1 orbitals are the $3d_{xy}$ and $3d_{x^2-y^2}$
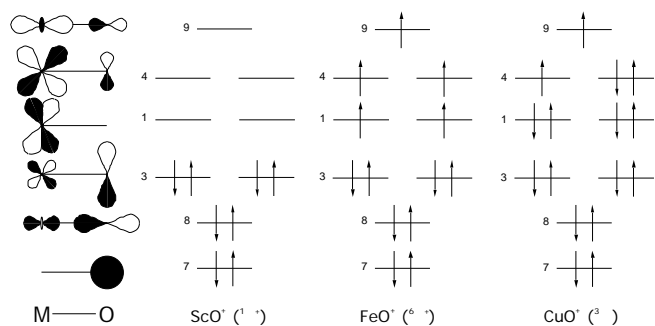
Figure 2: Schematic molecular orbitals of MO^+

orbitals on the metal and are nonbonding. As expected, filling these orbitals has little effect on the M^+-O bond strength. The 4π and 9σ orbitals are the antibonding counterparts of the 3π and 8σ, with most of the electron density on the metal. Filling these orbitals progressively weakens the M^+-O bond, as is seen in Figure 1. The metal oxides with favorable thermodynamics for methane activation tend to have high-spin ground states, which has a profound effect on their reactivity.

Calculations and Reaction Mechanism

A detailed mechanism for the conversion of methane to methanol by MO^+ has been developed after extensive calculations. This mechanism includes two key concepts: concerted reaction involving the key $[HO-M-CH_3]^+$ insertion intermediate and, for most metals, two-state reactivity. Figure 3 shows a schematic potential energy surface for the conversion of methane to methanol by FeO^+. This is an extension of extensive calculations at the B3LYP/6-311G(d,p) level by Yoshizawa et al. on methane activation by FeO^+ (36, 37) and the other first-row metals.(38, 39) Schröder et al.(40) and Fiedler et al.(19) have also carried out calculations on methane-methanol conversion by FeO^+ and the late first-row transition metals, respectively. In the figure the solid line indicates the sextet (high-spin) reaction path, the quartet path is in short dashes, and the minor pathway leading to
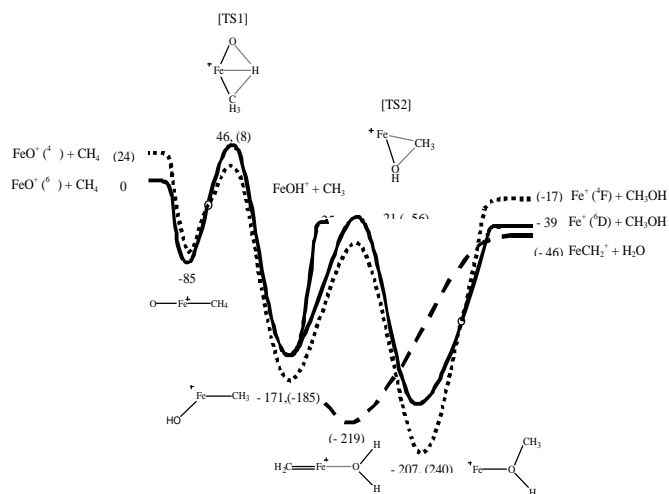

Figure 3: Schematic potential energy surface for the FeO^+ + CH_4 reaction

$FeCH_2^+$ + H_2O is in long dashes. The relative energies of reactants and products are based on established thermodynamics,(13) the energies of intermediates are based on our calculations(26, 41) at the B3LYP/6-311+G(d,p) level, and the energies of transition states, relative to the previous intermediate calculated by Yoshizawa et al.(38) are given. All energies are in kJ/mol; calculated energies include zero-point energy and thus correspond to 0 Kelvin values. Energies for the quartet surface are in parentheses.

The reaction proceeds as follows: electrostatic interaction between FeO^+ and methane produces the $[OFe\ CH_4]^+$ entrance channel complex. Depending on the level of theory, the Fe coordinates to either two (quartet state, and sextet state at B3LYP/6-311G(d,p)) or three (sextet state at B3LYP/6-311+G(d,p)) hydrogens. In a classical case of back-bonding, the iron pulls electron density from the C-H σ bonding orbital and donates electrons to a Fe-C bonding, C-H anti-bonding orbital, weakening the C-H bond. At transition state TS1 the strong C-H bond in methane is being replaced by two bonds: a strong O-H bond and a fairly weak Fe-C bond. Although the reactants are

high-spin, at TS1 the low-spin state is significantly energetically favored. TS1 leads to the key insertion intermediate [HO–Fe–CH$_3$]$^+$, which can dissociate to produce FeOH$^+$ + CH$_3$ or can undergo migration of a methyl group (TS2) to produce the iron/methanol exit channel complex [Fe(CH$_3$OH)]$^+$, which subsequently dissociates. Calculations performed by Schröder et al.[40] at the MP2/ECP-DZ level of theory suggest that the minor FeCH$_2^+$ + H$_2$O product channel is derived from the dissociation of an aquo iron carbene intermediate [H$_2$C=Fe–OH$_2$]$^+$ which is separated from the insertion intermediate by a substantial barrier.

The potential energy surface shown in Figure 3 allows us to make several predictions about this reaction. First, although both reactants and products are high spin, at thermal energies the reaction occurs through low-spin intermediates.[37] In the figure, spin crossings are schematically indicated by circles. This "two-state reactivity" has been extensively studied by Shaik and coworkers, especially in the exothermic but very inefficient FeO$^+$ + H$_2$ → Fe$^+$ + H$_2$O reaction.[42-45] The *efficiency* of the reaction is determined by the energy of TS1 on the quartet surface, as well as by the lifetime of the [OFe·CH$_4$]$^+$ entrance channel complex, which determines the likelihood of a transition to the quartet surface. The low efficiency of the FeO$^+$ + H$_2$ reaction is due to the short lifetime of the entrance channel complex. In general, the *selectivity* of the reaction between M$^+$ + CH$_3$OH (methanol) and MOH$^+$ + CH$_3$ (methyl radical) products is primarily determined by the energy of TS2 relative to methyl radical products. Because MOH$^+$ is produced by simple bond fission of the insertion intermediate, it is entropically favored over the methanol channel, which occurs through the tighter transition state TS2. Thus, if TS2 is at an energy close to or above methyl products, the reaction will overwhelmingly produce MOH$^+$ + CH$_3$, as is observed for MnO$^+$. Similarly, in the iron system, where TS2 lies somewhat below

methyl radical products, the two pathways are competitive, but increased translational energy strongly favors the methyl radical pathway.[46]

In a classical dynamics study of methane-methanol conversion by FeO$^+$ Yoshizawa et al.[47] calculated that both the initial hydrogen abstraction that leads to [HO–Fe–CH$_3$]$^+$ and the methyl migration that produces [Fe(CH$_3$OH)]$^+$ occur in a concerted manner in 100 fs. This result was obtained using classical trajectories, starting from transition states TS1 and TS2. This result is misleading, as the bimolecular FeO$^+$ + CH$_4$ reaction is probably 2-4 orders of magnitude slower at thermal energies due to the time it takes for the entrance channel complex to randomly explore many configurations until it achieves the geometry of TS1 and for the insertion intermediate to reach TS2.

Based on analogy with FeO$^+$, a two-step concerted mechanism for methane-methanol conversion has also been proposed for Fe-doped zeolites[48] and the oxidizing enzyme cytochrome P450.[49] In a series of papers Yoshizawa and coworkers have also advocated this mechanism for the enzyme soluble methane monooxygenase,[50-54] although a non-concerted radical mechanism is favored by others.[55, 56]

Methane Activation by MO$^+$: Reaction Studies

Metals that, based on thermodynamics, could potentially catalytically convert methane to methanol are shown in bold in Figure 1. The reactions of many of these metal oxide cations have been investigated experimentally, and the results are summarized in Table 1. Results are mostly based on single-collision, thermal reactions in an ICR cell, complemented by single-collision guided ion beam studies in which the collision energy can be varied (FeO$^+$ and CoO$^+$) and multiple-collision thermal flow tube studies (SIFT) (FeO$^+$). Many of these results have been discussed by Schröder, Schwarz and coworkers in a series of reviews.[15, 57-59]

MO$^+$	% Efficiency	M$^+$ + CH$_3$OH	MOH$^+$ + CH$_3$	MCH$_2^+$ + H$_2$O
MnO$^+$	40	< 1	100	-
FeO$^+$ (a)	20	41	57	2
FeO$^+$ (b)	9	39	61	trace
FeO$^+$ (c)	7	18	82	-
CoO$^+$	0.5	100	-	-
NiO$^+$	20	100	-	-
PtO$^+$	100	25	-	75

<u>Table 1:</u> Reactions of MO$^+$ with methane. Values are from (59), except a) 1990 ICR study(12); b) 1997 ICR study(46); c) 1997 SIFT study(46)

We'll discuss the reactivity of the highlighted metal oxides in order. CrO$^+$ does not react with methane under thermal conditions.(60) This is not surprising, as the reaction of the quartet ground state of CrO$^+$ to produce ground state sextet Cr$^+$ is spin-forbidden, and transition state TS1 is calculated to lie barely below the reactants. The alternate CrOH$^+$ + CH$_3$ channel is calculated to be quite endothermic.(39) MnO$^+$ reacts quite efficiently with methane, but produces MnOH$^+$ + CH$_3$ almost exclusively.(61) As Yoshizawa points out, the reaction is efficient because TS1 lies 28 kJ/mol below the reactants, and MnOH$^+$ is the preferred product because it lies only slightly above TS2.(39)

Since the original report that gas-phase FeO$^+$ directly converts methane to methanol,(12) this reaction has been the subject of several studies.(40, 46, 62) Three groups have collaborated in a critical study of this reaction over a range of pressures and collision energies.(46) First, under single-collision conditions at thermal energies, they revised the original estimate of the reaction efficiency of 20% down to 9%. This modest efficiency is consistent with Figure 3, which shows that TS1 for the high-spin sextet state lies well above the reactant energies, requiring the encounter complex to undergo a transition to the low-spin (quartet) state if it is to react, and TS1 on the quartet surface lies only slightly below the reactants. The branching ratio between the methanol and methyl radical pathways

depends on pressure and also strongly on collision energy. This competition reflects the relative energies of TS2 and the FeOH$^+$ products. When compared to the single collision ICR studies, the SIFT experiments, which are carried out at 0.5 mbar pressure (corresponding to a collision rate of ~10^8 s^{-1}), find an increased propensity to produce methanol. This is likely due to collisions removing energy from the reaction complex, favoring the more thermodynamically stable methanol product.(46) Ions with the [FeCH$_4$O]$^+$ stoichiometry were not observed in this study, suggesting that there were too few collisions to cool the complex below the energy required to produce methanol. These results suggest that the thermal FeO$^+$ + CH$_4$ reaction takes place in 10^{-10}-10^{-8} s. Single-collision guided ion beam experiments(46) show that increased collision energy dramatically favors the FeOH$^+$ channel (by 99:1 at 0.7 eV), reflecting that this channel is entropically favored.

As for the remaining first-row metals, an ICR study finds that CoO$^+$ reacts very inefficiently with methane at thermal energies,(59) while a guided ion beam study finds essentially no methanol production below 0.6 eV collision energy.(63) The reaction of the quintet ground state of CoO$^+$ to produce ground state triplet Co$^+$ is spin forbidden, and TS1 is calculated to lie 23 kJ/mol (triplet) and 45 kJ/mol (quintet) above the reactants.(39) It is likely that the small reactivity observed in the ICR study is due to

contamination by metastable triplet states of CoO^+ which are calculated to lie near 1 eV.(19) NiO^+ reacts efficiently with methane to produce methanol. TS1 (low-spin) is calculated to lie 15 kJ/mol below reactants, which is consistent with good efficiency, and TS2 lies well below $NiOH^+$ products, suggesting a strong preference for methanol production.(39) Yoshizawa has suggested that CuO^+ should react very efficiently and selectively to convert methane to methanol, but the Cu^+-O bond is so weak that even reaction of Cu^+ with N_2O is endothermic, so the difficulty of producing CuO^+ has, so far, precluded its study.

Of the heavier metals that are highlighted, only the reaction of PtO^+ with methane has been studied. PtO^+ reacts with methane at the collision rate, producing $Pt^+ + CH_3OH$ and $PtCH_2^+ + H_2O$ in a 25:75 ratio.(64) Production of MCH_2^+ which is, at best, a very minor pathway for the first-row metals, is due to the exceptionally strong bonds third-row transition metals form with methylene, due to relativistic effects.(23, 65) The strong Pt^+-CH_2 bond means that bare Pt^+ activates methane, leading to a catalytic cycle in which Pt^+ converts methane to methanol and formaldehyde in the presence of oxygen.(66) The potential energy surface for these reactions has also been investigated in detail.(66)

Spectroscopy of Reaction Intermediates

The potential energy surface for the $FeO^+ + CH_4$ reaction features three distinct intermediates (Fig. 3). If these intermediates are formed and cooled, they should be stable in the absence of collisions and they can be studied. In an elegant series of experiments Schröder et al. produced these intermediates by reacting Fe^+ with organic precursors in an ICR cell. The intermediates were identified based on fragment ions produced by collision-induced dissociation.(40) In our laboratory, we produce the $[HO–Fe–CH_3]^+$ and $[H_2O\text{-}Fe=CH_2]^+$ intermediates using specific ion-molecule reactions,
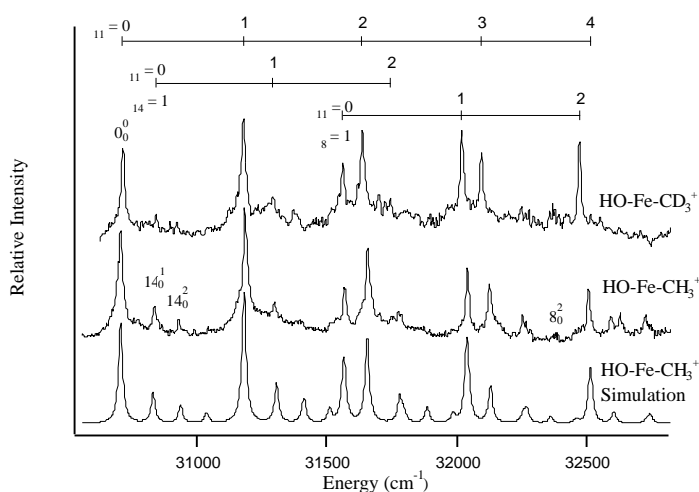

Figure 4: Photodissociation spectra of insertion intermediates of the $FeO^+ + CH_4$ reaction

cool them in a supersonic expansion, and measure their photodissociation spectrum. Details on the technique, ion characterization, and results on $[H_2O\text{-}Fe=CH_2]^+$ are given elsewhere.(26, 41) The photodissociation spectra of $[HO–Fe–CH_3]^+$ and $[HO–Fe–CD_3]^+$ obtained by monitoring $FeOH^+$ are shown in Figure 4. As these intermediates are probably in the sextet state,(41) the structure is due to vibrations in an electronically excited sextet state of the intermediate. This structure has been assigned to an extended progression in the Fe-C stretch (ν_{11}) and short progressions in the Fe-O stretch (ν_8) and O-Fe-C bend (ν_{14}). Extensive calculations(41) and the simulation shown in the figure support this assignment. Photodissociation of the insertion intermediate produces $Fe^+ + CH_3OH$ and $FeOH^+ + CH_3$ in a 44:56 ratio at each peak. Photodissociation away from a peak gives increased production of the non-reactive $FeOH^+$ channel (33:67 ratio). So, photoexcitation of the $[HO–Fe–CH_3]^+$ intermediate triggers the $FeO^+ + CH_4$ reaction, leading to the same products as are observed in the bimolecular reaction.

We have calculated the RRKM dissociation rate for excited $[HO–Fe–CH_3]^+$ using frequencies calculated at the B3LYP/6-31G(d,p) level for TS2 and a loose transition state for $FeOH^+$

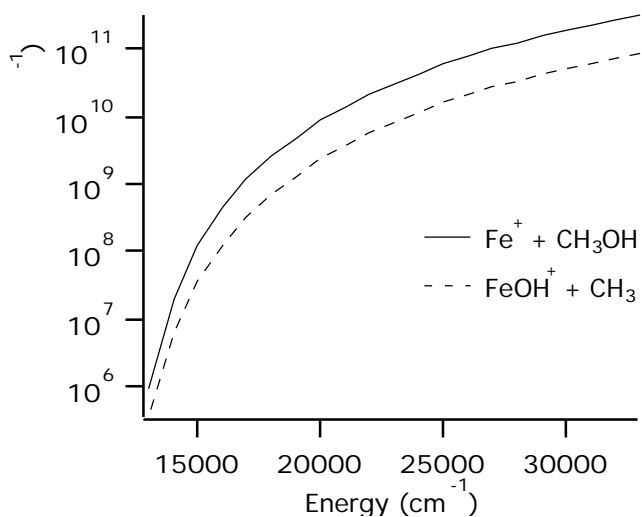Figure 5: Calculated dissociation rate of the energized $[HO-Fe-CH_3]^+$ intermediate

the $FeOH^+ + CH_3$ products lie ~146 kJ/mol (~12500 cm^{-1}) above $[HO–Fe–CH_3]^+$. Figure 5 shows calculated RRKM rates for the loss of methanol and methyl radical using these energetics (all energies are relative to the sextet state of $[HO–Fe–CH_3]^+$). The results are in qualitative agreement with our observations in that the two product channels are competitive, but predicts more Fe^+ than $FeOH^+$. This could be due to incorrect relative energies for the two channels (shifting TS2 40 kJ/mol to higher energy gives a branching ratio in agreement with experiment), or to the calculation of several very low vibrational frequencies for TS2. Raising these frequencies results in a much tighter TS2 and less Fe^+ production.

Acknowledgements

production.(26, 41) This calculation assumes that the electronically excited complex relaxes to vibrationally excited molecules in the ground electronic state, which then dissociate. This assumption is supported by the long lifetime of the excited complex, evidenced by the resolved vibrational and partially resolved rotational structure in the spectrum. Figure 3 shows that both TS2 and

References

1. J. Haggin, Chem. & Eng. News **71**, 27 (1993).
2. R. H. Crabtree, Chem. Rev. **95**, 987 (1995).
3. B. K. Warren and S. T. Oyama, *Heterogeneous Hydrocarbon Oxidation* (American Chemical Society, Washington, D.C., 1996).
4. Y. Wang and K. Otsuka, J. Chem. Soc. Chem. Commun. **1994**, 2209 (1994).
5. Y. Wang, K. Otsuka and K. Ebitani, Catal. Lett. **35**, 259 (1995).
6. H. Matsumoto, S. Tanabe, K. Okitsu, Y. Hayashi and S. L. Suib, J. Phys. Chem. A **105**, 5304 (2001).
7. R. A. Periana, D. J. Taube, S. Gamble, H. Taube, T. Satoh and H. Fujii, Science **280**, 560 (1998).
8. R. Raja and P. Ratnasamy, Appl. Catal. A General **158**, L7 (1997).
9. J. Haggin, Chem. & Eng. News **72**, 24 (1994).
10. A. C. Rosenzweig, C. A. Frederick, S. J. Lippard and P. Nordlund, Nature **366**, 537 (1993).
11. L. J. Shu, J. C. Nesheim, K. Kauffmann, E. Munck, J. D. Lipscomb and L. Que, Science **275**, 515 (1997).
12. D. Schröder and H. Schwarz, Angew. Chem. Intl. Ed. Engl. **29**, 1433 (1990).
13. H. Y. Afeefy, J. F. Liebman and S. E. Stein, in *NIST Chemistry WebBook, NIST Standard Reference Database Number 69* , edited by W. G. Mallard, and P. J. Linstrom (National

Institute of Standards and Technology, Gaithersburg MD 20899, July 2001).

14. P. B. Armentrout and B. L. Kickel, in *Organometallic Ion Chemistry*, edited by B. S. Freiser (Kluwer Academic Publishers, Dordrecht, The Netherlands, 1994).

15. D. Schröder, H. Schwarz and S. Shaik, Struct. Bonding **97**, 91 (2000).

16. X. G. Zhang and P. B. Armentrout, personal communication (2001).

17. J. F. Harrison, Chem. Rev. **100**, 679 (2000).

18. E. A. Carter and W. A. Goddard III, J. Phys. Chem. **92**, 2109 (1988).

19. A. Fiedler, D. Schröder, S. Shaik and H. Schwarz, J. Am. Chem. Soc. **116**, 10734 (1994).

20. M. Sodupe, V. Branchadell, M. Rosi and C. W. Bauschlicher Jr., J. Phys. Chem. A **101**, 7854 (1997).

21. Y. Nakao, K. Hirao and T. Taketsugu, J. Chem. Phys. **114**, 7935 (2001).

22. A. Fiedler, J. Hrusák, W. Koch and H. Schwarz, Chem. Phys. Lett. **211**, 242 (1993).

23. C. Heinemann, W. Koch and H. Schwarz, Chem. Phys. Lett. **245**, 509 (1995).

24. T. Borowski and E. Broclawik, Chem. Phys. Lett. **339**, 433 (2001).

25. F. Aguirre, C. J. Thompson and R. B. Metz, manuscript in preparation (2002).

26. F. Aguirre, Ph.D. Thesis, University of Massachusetts, 2002.

27. C. J. Thompson, F. Aguirre, K. L. Stringer and R. B. Metz, manuscript in preparation (2002).

28. J. M. Dyke, B. W. J. Gravenor, M. P. Hastings and A. Morris, J. Phys. Chem. **89**, 4613 (1985).

29. J. M. Dyke, B. W. J. Gravenor, R. A. Lewis and A. Morris, J. Chem. Soc. Faraday Trans. 1 **79**, 1083 (1983).

30. J. M. Dyke, A. M. Ellis, M. Feher, A. Morris, A. J. Paul and J. C. H. Stevens, J. Chem. Soc. Faraday Trans. II **83**, 1555 (1987).

31. A. D. Sappey, G. Eiden, J. E. Harrington and J. C. Weisshaar, J. Chem. Phys. **90**, 1415 (1989).

32. J. Harrington and J. C. Weisshaar, J. Chem. Phys. **97**, 2809 (1992).

33. J. Husband, F. Aguirre, P. Ferguson and R. B. Metz, J. Chem. Phys. **111**, 1433 (1999).

34. A. Kamariotis, T. Hayes, D. Bellert and P. J. Brucat, Chem. Phys. Lett. **316**, 60 (2000).

35. P. J. Brucat, personal communication (2001).

36. K. Yoshizawa, Y. Shiota and T. Yamabe, Chem. Eur. J. **3**, 1160 (1997).

37. K. Yoshizawa, Y. Shiota and T. Yamabe, J. Chem. Phys. **111**, 538 (1999).

38. K. Yoshizawa, Y. Shiota and T. Yamabe, J. Am. Chem. Soc. **120**, 564 (1998).

39. Y. Shiota and K. Yoshizawa, J. Am. Chem. Soc. **122**, 12317 (2000).

40. D. Schröder, A. Fiedler, J. Hrusák and H. Schwarz, J. Am. Chem. Soc. **114**, 1215 (1992).

41. F. Aguirre, J. Husband, C. J. Thompson, K. L. Stringer and R. B. Metz, J. Chem. Phys. **116**, 4071 (2002).

42. D. Schröder, A. Fiedler, M. F. Ryan and H. Schwarz, J. Phys. Chem. **98**, 68 (1994).

43. M. Filatov and S. Shaik, J. Phys. Chem. A **102**, 3835 (1998).

44. D. Danovich and S. Shaik, J. Am. Chem. Soc. **119**, 1773 (1997).

45. D. Schröder, S. Shaik and H. Schwarz, Acc. Chem. Res. **33**, 139 (2000).

46. D. Schröder, H. Schwarz, D. E. Clemmer, Y. Chen, P. B. Armentrout, V. Baranov and D. K. Bohme, Int. J. Mass Spectrom. Ion Proc. **161**, 175 (1997).

47. K. Yoshizawa, Y. Shiota, Y. Kagawa and T. Yamabe, J. Phys. Chem. A **104**, 2552 (2000).

48. K. Yoshizawa, Y. Shiota, T. Yumura and T. Yamabe, J. Phys. Chem. B **104**, 734 (2000).

49. K. Yoshizawa, T. Kamachi and Y. Shiota, J. Am. Chem. Soc. **123**, 9806 (2001).

50. K. Yoshizawa, J. Biol. Inorg. Chem. **3**, 318 (1998).

51. K. Yoshizawa, T. Ohta and T. Yamabe, Bull. Chem. Soc. Jpn. **71**, 1899 (1998).

52. K. Yoshizawa, J. Inorg. Biochem. **74**, 58 (1999).

53. K. Yoshizawa, J. Inorg. Biochem. **78**, 23 (2000).

54. K. Yoshizawa, A. Suzuki, Y. Shiota and T. Yamabe, Bull. Chem. Soc. Jpn. **73**, 815 (2000).

55. P. E. M. Siegbahn and R. H. Crabtree, Struct. Bonding **97**, 125 (2000).

56. H. Basch, D. G. Musaev, K. Mogi and K. Morokuma, J. Phys. Chem. A **105**, 3615 (2001).

57. H. Schwarz and D. Schröder, Pure Appl. Chem. **72**, 2319 (2000).

58. K. Eller and H. Schwarz, Chem. Rev. **91**, 1121 (1991).

59. D. Schröder and H. Schwarz, Angew. Chem. Int. Ed. Engl. **34**, 1973 (1995).

60. H. Kang and J. L. Beauchamp, J. Am. Chem. Soc. **108**, 7502 (1986).

61. M. F. Ryan, A. Fiedler, D. Schröder and H. Schwarz, J. Am. Chem. Soc. **117**, 2033 (1995).

62. M. Brönstrup, D. Schröder and H. Schwarz, Chem. Eur. J. **5**, 1176 (1999).

63. Y.-M. Chen, D. E. Clemmer and P. B. Armentrout, J. Am. Chem. Soc. **116**, 7815 (1994).

64. C. Heinemann, R. Wesendrup and H. Schwarz, Chem. Phys. Lett. **239**, 75 (1995).

65. C. Heinemann, R. H. Hertwig, R. Wesendrup, W. Koch and H. Schwarz, J. Am. Chem. Soc. **117**, 495 (1995).

66. M. Pavlov, M. R. A. Blomberg, P. E. M. Siegbahn, R. Wesendrup, C. Heinemann and H. Schwarz, J. Phys. Chem. A **101**, 1567 (1997).